Inorg. Chem. **2006**, *45*, 10270–10276

Inorganic Chemistry Article

Electrical Conducting Bis(Oxalato)platinate Complex with Direct Connection of Cu^{II} Ions

Chihiro Yamamoto,[†] Hiroyuki Nishikawa,[†] Masayuki Nihei,[†] Takuya Shiga,[†] Masato Hedo,[‡] Yoshiya Uwatoko,[‡] Hiroshi Sawa,[§] Hiroshi Kitagawa,[||] Yasujiro Taguchi,[⊥] Yoshihiro Iwasa,[⊥] and Hiroki Oshio*,[†]

Graduate School of Pure and Applied Sciences, University of Tsukuba, 1-1-1 Tennoudai, Tsukuba, Ibaraki 305-8571, Japan, The Institute for Solid State Physics, The University of Tokyo, 5-1-5 Kashiwanoha, Kashiwa, Chiba 277-8581, Japan, Photon Factory, Institute of Materials Structure Science, High Energy Accelerator Research Organization, 1-1 Oho, Tsukuba, Ibaraki 305-0801, Japan, Department of Chemistry, Faculty of Science, Kyushu University, 6-10-1 Hakozaki, Higashi-ku, Fukuoka 812-8581, Japan, and Institute for Materials Research, Tohoku University, 2-1-1 Katahira, Aoba-ku, Sendai 980-8577, Japan

Received May 8, 2006

Reactions of $K_{1.62}[Pt(ox)_2]\cdot 2H_2O$ and $[Cu(bpy)(H_2O)_3](NO_3)_2$ yielded partially oxidized one-dimensional (1D) bis(oxalato)platinates of $[Cu(bpy)(H_2O)_n]_6[Pt(ox)_2]_7\cdot 7H_2O$ ($n = 2$, 3, or 4) (**1**) and $[Cu(bpy)(H_2O)_n]_8[Pt(ox)_2]_{10}\cdot 8H_2O$ ($n = 3$ or 4) (**2**). The average oxidation numbers of the platinum ions in **1** and **2** are +2.29 and +2.40, respectively. Complexes **1** and **2** crystallize in the triclinic $P\bar{1}$ and monoclinic $C2/c$ space groups, respectively, and the $[Pt(ox)_2]^{n-}$ anions are stacked along the crystallographic b axis with 7-fold periodicity for **1** and 10-fold periodicity for **2**. In **1**, an oxalato ligand in the platinum chain directly coordinates to a paramagnetic $[Cu(bpy)(H_2O)_3]^{2+}$ ion, whereas no such direct coordination was observed for **2**. The electrical conductivity of **2** at room temperature along the platinum chain is approximately 3 orders of magnitude smaller ($\sigma_{||} = 1.3 \times 10^{-3}$ S cm^{-1}) than that of **1** ($\sigma_{||} = 0.9$–0.5 S cm^{-1}), and the activation energies of **1** and **2** are 29 and 67 meV, respectively. The longest inter-platinum distances in **1** and **2** are 2.762 and 3.0082 Å, respectively, and this is responsible for the lower electrical conductivity of **2**. An X-ray oscillation photograph taken along the b axis of **1** reveals the 7-fold periodicity in the 1D chain, consistent with the period of the Peierls distortion estimated from the degree of partial oxidation. The semiconducting state of **1** can therefore be regarded as a commensurate Peierls state. The magnetoresistance of **1** at ambient pressure indicates no interaction between conduction electrons in the platinum chain and local spins of the paramagnetic Cu^{II} ions. Application of hydrostatic pressures of up to 3 GPa enhances electrical conduction, as is often seen as the usual pressure effect on the electrical conductivity, which is due to enhanced orbital (Pt-5d$_{z^2}$) overlap by pressure application.

Introduction

In the last several decades, the issue of low dimensionality in solid-state physics has been focused on due to the unique physical properties.[1] The optical and conductive properties of halogen-bridged metal complexes have been investigated from the viewpoint of strong electron correlation.[2] Partially oxidized tetracyanoplatinates ($M_x[Pt(CN)_4]\cdot nH_2O$)[3] and bis(oxalato)platinates ($M_x[Pt(ox)_2]\cdot nH_2O$)[4] are one series of

* To whom correspondence should be addressed. E-mail: oshio@chem.tsukuba.ac.jp.
† University of Tsukuba.
‡ The University of Tokyo.
§ High Energy Accelerator Research Organization.
|| Kyushu University.
⊥ Tohoku University.

(1) (a) *Organic and Inorganic Low-Dimensional Crystalline Materials*; Delhaes, P., Drillon, M., Eds.; Plenum Press: New York, 1987. (b) *Physics and Chemistry of Low-dimensional inorganic conductors*; Schelnker, C., Ed.; Plenum Press: New York, 1996. (c) Kagoshima, S.; Nagasawa, H.; Sambongi, T. *One-dimensional Conductors*; Springer-Verlag: Berlin, 1988.
(2) (a) Kitagawa, H.; Mitani, T. *Coord. Chem. Rev.* **1999**, *190*−*192*, 1169−1184. (b) Yamashita, M.; Manabe, T.; Kawashima, T.; Okamoto, H.; Kitagawa, H. *Coord. Chem. Rev.* **1999**, *190*−*192*, 309−330. (c) Kishida, H.; Matsuzaki, H.; Okamoto, H.; Manabe, T.; Yamashita, M.; Taguchi, Y.; Tokura, Y. *Nature (London)* **2000**, *405*, 929−932.

10.1021/ic0607742 CCC: $33.50

Published on Web 11/15/2006

pioneer materials for such low-dimensional conductors, and one-dimensional (1D) electrical properties associated with Peierls instability have been extensively studied. The electrical conducting properties of 1D platinates, particularly $K_2[Pt(CN)_4]Br_{0.3}\cdot 2H_2O$ (KCP),[5] are well understood from the degree of partial oxidation (DPO). It has been pointed out that the nonmetallic region at low temperature is a charge-density-wave (CDW) state.[6] The nature of the metal-to-insulator transition of $M_x[Pt(ox)_2]\cdot nH_2O$ is, on the other hand, much more complicated than that of KCP; in addition to the simple Peierls transition, the ordering of cations also opens a gap at the Fermi level, depending on the M^+ ions.[7] Incorporation of paramagnetic ions to the electrical conducting 1D chain of $[Pt(ox)^2]^{n-}$ has been reported for $M_x[Pt(ox)_2]\cdot nH_2O$ ($M = Ni^{II}$,[9,10] Co^{II},[11] Fe^{II},[7] Mn^{II},[9] or Cu^{II}[12]). However, no direct coordination of the paramagnetic metal ions to oxalate has been observed so far. An oxalate is used to construct a two- or three-dimensional molecular framework of molecular-based magnets,[8] and oxalato complexes can be used to construct materials having multiple functions including conductivity and magnetism. We report herein the first partially oxidized $[Pt(ox)_2]^{n-}$ complex with a paramagnetic Cu^{II}−bipyridine complex linking to the conducting chain (Chart 1). The syntheses, crystal structures, and transport properties under pressures of up to 3 GPa and magnetic fields of up to 9 T are reported.

Chart 1

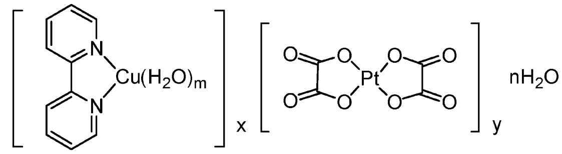

1: m = 2, 3, or 4, n = 7, x = 6, y = 7

2: m = 3 or 4, n = 8, x = 8, y = 10

Table 1. Crystallographic Data for Complexes **1** and **2**

	1	2
formula	$C_{88}H_{67}Cu_6N_{12}O_{82}Pt_7$	$C_{60}H_{44}Cu_4N_8O_{58}Pt_5$
fw	4351.41	3034.64
cryst syst	triclinic	monoclinic
space group	$P\bar{1}$	$C2/c$
a (Å)	15.910(6)	14.580(3)
b (Å)	19.772(8)	25.614(6)
c (Å)	20.594(8)	22.270(5)
α (deg)	78.283(6)	
β (deg)	73.745(6)	99.109(4)
γ (deg)	71.742(7)	
V (Å^3)	5859(4)	8212(3)
Z	2	4
T (K)	200	200
radiation (Å)	0.71073	0.71073
ρ_{calcd} (g cm^{-3})	2.467	2.455
μ/cm^{-1}	9.512	9.619
F(000)	4110	5720
residuals:[a] R1; wR2	0.0427; 0.1004	0.0439; 0.0891

[a] $R1 = \sum||F_o| - |F_c||/\sum|F_o|$. $wR2 = [\sum[w(F_o^2 - F_c^2)^2]/\sum[w(F_o^2)^2]]^{0.5}$.

Experimental Section

Synthesis. All chemicals were used as received without further purification. $[Cu(bpy)(H_2O)_3](NO_3)_2$ was prepared according to literature methods.[13] Partially oxidized $K_{1.62}[Pt(ox)_2]\cdot 2H_2O$ was obtained by oxidizing $K_2[Pt(ox)_2]$ with K_2PtCl_6 according to the method reported previously.[14]

$[Cu(bpy)(H_2O)_n]_6[Pt(ox)_2]_7\cdot 7H_2O$ (n = 2, 3, or 4) (1). An aqueous solution (10 mL) of complex $[Cu(bpy)(H_2O)_3](NO_3)_2$ (18 mg, 0.045 mmol) was added to an aqueous solution (20 mL) of $K_{1.62}[Pt(ox)_2]\cdot 2H_2O$ (33 mg, 0.07 mmol) with stirring. The reaction mixture was allowed to stand undisturbed at room temperature for 1 day, and black pillar-shaped crystals of **1** were precipitated with dark blue needles of $[Cu(bpy)(H_2O)_n]_8[Pt(ox)_2]_{10}\cdot 8H_2O$ ($n = 3$ or 4) (**2**) as the minor product. The sample crystals for physical measurements were maintained in the mother liquor to avoid loss of the water of crystallization.

X-ray Crystallography. Single crystals of **1** and **2** were mounted with epoxy resin on the tip of a glass fiber. Diffraction data were collected at 200 K on a Bruker SMART APEX diffractometer fitted with a CCD-type area detector, and a full sphere of data was collected using graphite-monochromated Mo Kα radiation (λ = 0.71073 Å). The first 50 frames of data were recollected to ensure that the crystal had not deteriorated during data collection. Data frames were integrated with the SAINT program and merged to give a unique data set for structure determination. Absorption correction by integration was applied on the basis of measured indexed crystal faces using XPREP. The structure was solved by direct methods and refined by the full-matrix least-squares method on F^2 data with the SHELXTL 5.1 package (Bruker Analytical X-ray Systems). All non-hydrogen atoms were refined with anisotropic thermal parameters. Hydrogen atoms were included in calculated positions and refined with isotropic thermal parameters riding on those of the parent atoms. Crystallographic data and structure refinement details are listed in Table 1.

To observe superlattice reflections, oscillation photographs were taken at room temperature with the oscillation range of 6° and

(3) Miller, J. S.; Epstein, A. *Prog. Inorg. Chem.* **1976**, *20*, 1−151. (b) Williams, J. M.; Schultz, A. J.; Undrehill, A. E.; Carneiro, K. In *Extended Linear Chain Compounds*; Miller, J. S., Ed.; Plenum Press: New York, 1982; pp 73−118.

(4) (a) Krogmann, K. *Angew. Chem., Int. Ed. Engl.* **1969**, *8*, 35−42. (b) Undrehill, A. E.; Watkins, D. M.; Williams, J. M.; Carneiro, K. In *Extended Linear Chain Compounds*; Miller, J. S., Ed.; Plenum Press: New York, 1982; pp 119−156.

(5) Comès, R.; Lambert, H.; Launois, H.; Zeller, H. R. *Phys. Rev. B* **1973**, *8*, 571−575.

(6) (a) Eagan, C. F.; Werner, S. A.; Saillant, R. B. *Phys. Rev. B* **1975**, *12*, 2036−2041. (b) Lynn, J. W.; Iizumi, M.; Shirane, G. *Phys. Rev. B* **1975**, *12*, 1154−1166.

(7) (a) Braude, A.; Lindegaard-Andersen, A.; Carneiro, K.; Petersen, A. S. *Solid State Commun.* **1980**, *33*, 365−369. (b) Braude, A.; Carneiro, K.; Jacobsen, C. S.; Mortensen, K.; Turner, D. J.; Underhill, A. E. *Phys. Rev. B* **1987**, *35*, 7835−7846.

(8) (a) Zhong, Z. J.; Matsumoto, N.; Okawa, H.; Kida, S. *Chem. Lett.* **1990**, 87−90. (b) Tamaki, H.; Zhong, Z. J.; Matsumoto, N.; Kida, S.; Koikawa, M.; Achiwa, N.; Hashimoto, Y.; Okawa, H. *J. Am. Chem. Soc.* **1992**, *114*, 6974−6979. (c) Decurtins, S.; Schmalle, H. W.; Oswald, H. R.; Linden, A.; Ensling, J.; Gütlich, P.; Hause, A. *Inorg. Chim. Acta* **1994**, *216*, 65−73. (d) Okawa, H.; Matsumoto, N.; Tamaki, H.; Ohba, M. *Mol. Cryst. Liq. Cryst.* **1993**, *233*, 257−262.

(9) Watkins, D. M.; Underhill, A. E.; Jacobsen, C. S. *J. Phys. Chem. Solids* **1982**, *43*, 183−187.

(10) Kobayashi, A.; Kiondo, H.; Sasaki, Y.; Kobayashi, H.; Underhill, A. E.; Watkins, D. M. *Bull. Chem. Soc. Jpn.* **1982**, *55*, 2074−2078.

(11) (a) Schultz, A. J.; Underhill, A. E.; Williams, J. M. *Inorg. Chem.* **1978**, *17*, 7, 1313−1318. (b) Bertinotti, A.; Luzet, D. *J. Phys. (Paris) Colloq.* **1983**, *39*, 1551−1554.

(12) Underhill, A. E.; Wood, D. J. In *Quasi One-Dimensional Conductors II, 1978 Vol. 96 of Lecture Notes in Physics*; Barisic, S., Bjelis, A., Cooper, J. R., Leontic, B., Eds.; Springer-Verlag: Berlin, 1979; pp 208−212.

(13) Jager, F. M.; Dijk, J. A. *Z. Anorg. Chem.* **1936**, *227*, 273−327.

(14) Krogmann, K.; Dode, P. *Chem. Ber.* **1966**, *99*, 3402−3407.

exposure time of 1 min using synchrotron radiation at the beam line BL1B of KEK-PF (High Energy Accelerator Research Organization, Photon Factory). The sample crystal was covered with Apiezon M to avoid loss of the water of crystallization and oriented in the b* direction perpendicular to the incident X-ray beam of 14.6 keV ($\lambda = 0.850$ Å).

Transport Measurements. Temperature dependences of resistance were measured between 50 and 290 K by the four-probe dc method, where the electrical current of 1 μA was applied along the Pt chain corresponding to the crystallographic b axis. Gold wires (10 μm) were used to contact carbon paste to a single crystal having a typical size of $0.5 \times 0.15 \times 0.1$ mm^3. The cooling or heating rate was approximately 0.3 K/min. Special care was given to the sampling because the water of crystallization is easily released from the crystal at room temperature, leading to deterioration of the crystal and lower electrical conductivity. The samples were attached to gold wires under cold nitrogen gas flow, and after wiring, the samples were covered with liquid paraffin to avoid loss of the water of crystallization. The reproducibility of the conductive behavior was checked for different samples. The resistance under high pressures was measured with a pressure-clamped cell having a double-cylindrical structure in the pressure range of 0.5−3 GPa with Daphne 7373 oil as pressure medium.[15] The magnetoresistance was measured with a Quantum Design Physical Property Measurement System (PPMS) under magnetic fields of up to 9 T at 100 K.

Results and Discussion

Synthesis. Reaction of partially oxidized $K_{1.62}[Pt(ox)_2]\cdot 2H_2O$ and $[Cu(bpy)(H_2O)_3](NO_3)_2$ yielded complex **1** as black pillar-shaped crystals. X-ray crystal analysis revealed that **1** has the chemical formula $[Cu(bpy)(H_2O)_n]_6[Pt(ox)_2]_7\cdot 7H_2O$ ($n = 2$, 3, or 4) and the formal oxidation number of the Pt ion is +2.29, whereas that of the Pt ion in $K_{1.62}[Pt(ox)_2]\cdot 2H_2O$ is +2.38. In addition to **1**, dark blue needles of $[Cu(bpy)(H_2O)_n]_8[Pt(ox)_2]_{10}\cdot 8H_2O$ ($n = 3$ or 4) (**2**) were obtained in the same reaction batch as the minor product. The ratio of the Cu to Pt ions in **2** is 0.8, suggesting the formal oxidation number of +2.40 for the Pt ion. Together, the results suggest that **2** is the product of the countercation exchange of $K_{1.62}[Pt(ox)_2]\cdot 2H_2O$.

Crystal Structure of Complex 1. Crystal structures of **1** are shown in Figure 1. Complex **1** crystallizes in triclinic space group $P\bar{1}$. The asymmetric unit is composed of seven (Pt1−Pt7) partially oxidized $[Pt(ox)_2]^{1.71-}$ anions, six (Cu1−Cu6) $[Cu(bpy)(H_2O)_n]^{2+}$ ($n = 2$, 3, or 4) cations, and seven water molecules. The averaged interatomic distances between Pt and O atoms of the seven crystallographically independent oxalato complexes range from 1.993 to 2.009 Å (Table 2), and they are almost identical within the standard derivation. This observation suggests that the platinum ions in the seven oxalato complexes have the averaged oxidation state of $Pt^{2.29+}$. The $[Pt(ox)_2]^{1.71-}$ anion is stacked along the crystallographic b axis with 7-fold periodicity. There are two 1D chains in the unit cell, which are related to the crystallographic inversion. In the chain, the oxalato oxygen atom in the Pt4 moiety coordinates directly to a Cu^{II} ion in $[Cu(bpy)(H_2O)_2]^{2+}$. It should be noted that this complex is the first example of 1D metal chain complexes based on bis(oxalato)platinates that are directly coordinated to the paramagnetic ion. In the chain, seven nonequivalent Pt ions have quasi-linear structures with the average Pt−Pt distance of 2.848 Å, and the oxalates are staggered with respect to those on the adjacent Pt ions. The torsion angle of the staggered configuration is approximately 60° except for the ligand on Pt4. The staggered angles of the oxalate ligand on Pt4 are 50° and 70°. Every other ligand is eclipsed except for $[Pt(ox)_2]^{1.71-}$ with Pt4, namely, conformational singularity exists at the Pt4 ion. The shortest Pt−Pt distance (2.762 Å) was observed for Pt4−Pt5 bonds, and this is slightly longer than the shortest inter-platinum distance found in $Rb_{1.67}[Pt(ox)_2]\cdot 1.5H_2O$ (2.717 Å) among partially oxidized platinate complexes.[16]

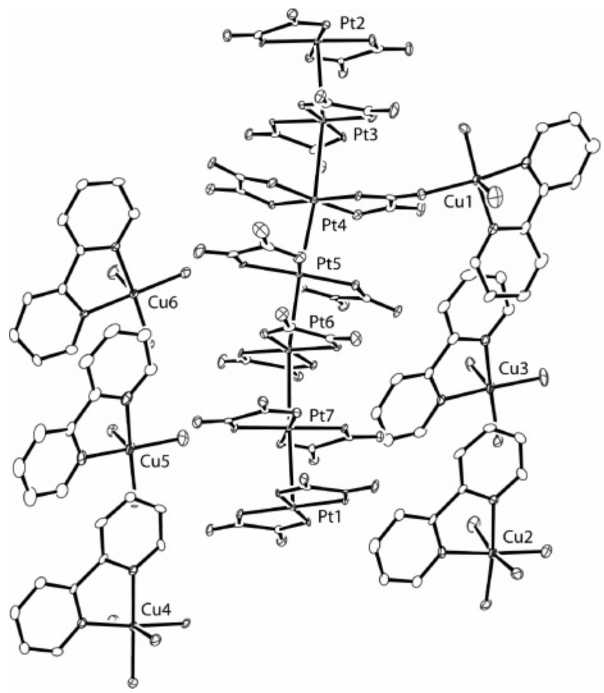

Figure 1. Asymmetric unit in the crystal structure of **1**. The inter-platinum Pt−Pt distances are Pt1−Pt2 = 2.904(1) Å, Pt2−Pt3 = 2.885(1) Å, Pt3−Pt4 = 2.879(1) Å, Pt4−Pt5 = 2.762(1) Å, Pt5−Pt6 = 2.800(1) Å, and Pt7−Pt1 = 2.855(1) Å.

Table 2. Selected Bond Distances (Å) for Complexes **1**

Pt(1)−O(1)	1.995(6)	Pt(4)−O(27)	2.007(6)
Pt(1)−O(2)	1.995(7)	Pt(4)−O(28)	2.010(7)
Pt(1)−O(3)	2.006(7)	Pt(4)···Pt(5)	2.762(1)
Pt(1)−O(4)	2.002(6)	Pt(5)−O(33)	1.997(7)
Pt(1)···Pt(2)	2.904(1)	Pt(5)−O(34)	1.988(6)
Pt(1)···Pt(7)	2.855(1)	Pt(5)−O(35)	2.005(6)
Pt(2)−O(9)	2.011(7)	Pt(5)−O(36)	1.980(7)
Pt(2)−O(10)	1.986(6)	Pt(5)···Pt(6)	2.779(1)
Pt(2)−O(11)	2.010(6)	Pt(6)−O(41)	1.990(6)
Pt(2)−O(12)	1.995(7)	Pt(6)−O(42)	1.993(7)
Pt(2)···Pt(3)	2.885(1)	Pt(6)−O(43)	1.999(6)
Pt(3)−O(17)	2.007(6)	Pt(6)−O(44)	2.007(6)
Pt(3)−O(18)	1.981(7)	Pt(6)···Pt(7)	2.800(1)
Pt(3)−O(19)	2.000(7)	Pt(7)−O(49)	2.001(7)
Pt(3)−O(20)	1.994(5)	Pt(7)−O(50)	2.002(6)
Pt(3)···Pt(4)	2.879(1)	Pt(7)−O(51)	1.990(6)
Pt(4)−O(25)	2.004(7)	Pt(7)−O(52)	1.996(7)
Pt(4)−O(26)	2.014(6)		

(15) Murata, K.; Yoshino, H.; Yadav, O. H.; Honda, Y.; Shirakawa, N. *Rev. Sci. Instrum.* **1997**, *68*, 2490−2493.

(16) Kobayashi, A.; Sasaki, Y.; Kobayashi, H. *Bull. Chem. Soc. Jpn.* **1979**, *52*, 3682−3691.

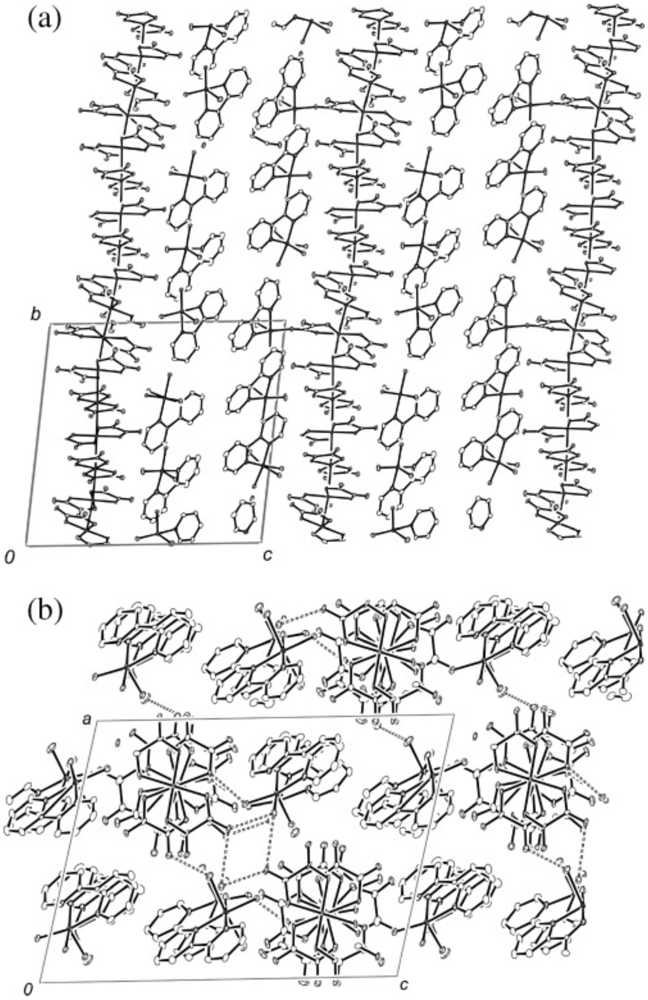

Figure 2. (a) Packing diagram for **1** projected along the *a* axis. (b) Crystal structure of **1** projected on the *ac* plane. Dashed lines represent hydrogen bonds among $[Cu(bpy)(H_2O)_n]^{2+}$, $[Pt(ox)_2]^{1.71-}$, and crystal water molecules.

In **1**, the platinum chains are surrounded by $[Cu(bpy)(H_2O)_n]^{2+}$ ($n = 2$, 3, or 4) and water molecules (Figure 2a), and there is no direct interaction among the chains. The Cu^{II} complexes are classified into three groups. Five coordination sites of Cu1, which is linked to the chain via the oxalate bridge, are occupied by two nitrogen atoms from bipyridine, one oxygen atom from oxalate, and two water molecules. Cu3, Cu5, and Cu6 ions have a square pyramidal coordination geometry composed of two nitrogen and three oxygen atoms from bipyridine and water molecules, respectively, whereas Cu2 and Cu4 have elongated octahedral coordination geometry (N_2O_6) with bipyridine coordinated from the equatorial position. It should be noted that the hydrogen bonds of water molecules with the terminal oxygen atoms of $[Pt(ox)_2]^{1.71-}$ connect the 1D platinum chains to form a two-dimensional network (Figure 2b).

To confirm the periodicity and investigate other superstructures accompanied by modulations such as incommensurate superstructures along the platinum chain direction, i.e., the crystallographic *b* direction, an X-ray oscillation photograph of **1** obtained by using synchrotron radiation was examined (Figure 3). The Bragg spots of the reciprocal lattice layers for $k = 7n$ are particularly strong, suggesting that the 7-fold periodicity exists in the 1D chain. Except for the Bragg spots corresponding to the 7-fold periodicity, neither a satellite peak nor a diffuse line was observed, suggesting no other superstructures exist.

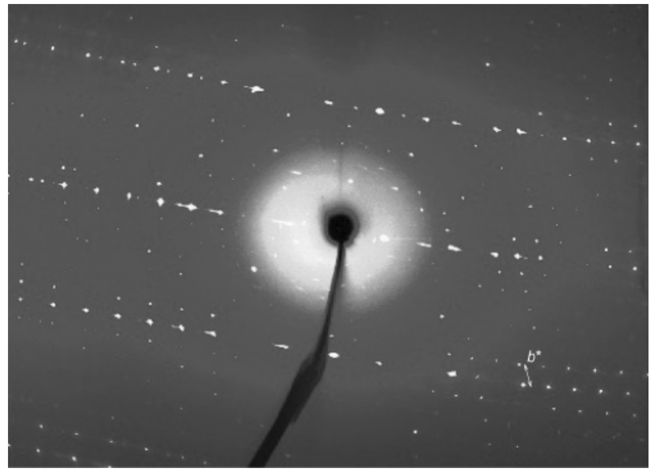

Figure 3. X-ray oscillation photograph of **1** taken at room temperature. Sample was oriented in the b^* direction perpendicular to the incident X-ray beam of 14.6 keV ($\lambda = 0.850$ Å).

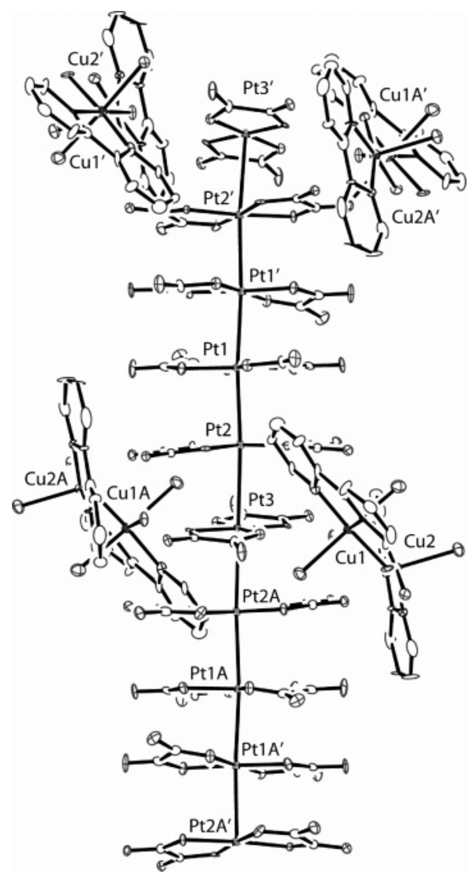

Figure 4. Crystal structure of **2** projected along the *a* axis.

Crystal Structure of Complex 2. **2** crystallizes in monoclinic space group *C*2/*c* (Figure 4). The unit cell contains two crystallographically independent $[Cu(bpy)(H_2O)_n]^{2+}$ cations, two water molecules, and three $[Pt(ox)_2]^{1.6-}$ anions, one of which locates on the inversion center. A crystallographic 2-fold axis passes through the center between Pt1 and Pt1′ perpendicularly to the platinum stackings. As a

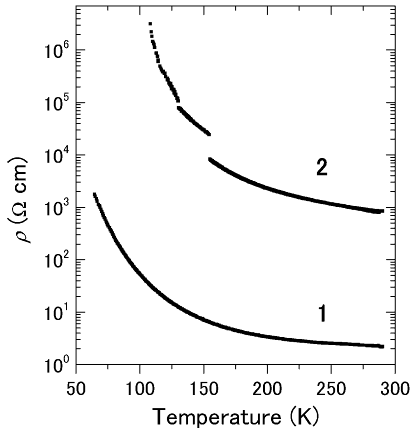

Figure 5. Temperature dependence of the resistivities of **1** and **2**.

result, platinum complexes form the 1D chain with 10-fold periodicity. Remarkable differences are noted between **1** and **2**: the Pt/Cu ratio suggests the average oxidation number of +2.4 for the Pt ion in **2**, which is close to the value (+2.38) of the starting material $K_{1.62}[Pt(ox)_2]\cdot 2H_2O$, and $[Cu(bpy)(H_2O)_n]^{2+}$ is not connected to the platinum chain via the oxalate bridge. The Pt−Pt distances in **2** are 2.7789 Å (Pt1−Pt2), 3.0082 Å (Pt2−Pt3), and 2.764 Å (Pt1−Pt1′), and the longest Pt−Pt distance in **2** is longer than that in **1** (2.904 Å). The Pt ions form the distorted chain with the oxalate ligands staggered with immediately adjacent complexes. The coordination geometries about Cu^{II} ions in $[Cu(bpy)(H_2O)_n]^{2+}$ (n = 3 or 4) are square pyramidal and octahedral, respectively, where bipyridine ligands coordinate at the equatorial positions.

Transport Properties of 1 at Ambient Pressure. The electrical resistivity of **1** along the 1D platinum chain direction ($\sigma_{\|}$) was measured in several samples. The electrical conductivity at room temperature varies from 0.9 to 0.03 S cm^{-1}. This is because the sample crystal easily loses water of crystallization, causing deterioration of the crystal and lower electrical conductivity. We estimated the conductivity of **1** at room temperature to be 0.9−0.5 S cm^{-1} by taking special care in sampling as described in the Experimental Section. The conductivity along the interchain direction ($\sigma_{\perp}$) is smaller than $\sigma_{\|}$ by 4 orders of magnitude, indicating a highly 1D character along the platinum chain direction. The resistivity of **1** as a function of temperature measured at ambient pressure showed semiconducting behavior without any anomalies (Figure 5) and can be well described by an activation-type formula, $\rho(T) = A \exp(\Delta E/k_BT)$, where A is a temperature-independent constant, k_B the Boltzmann constant, and ΔE the activation energy, suggesting that this salt is a band insulator with an activation energy of 29 meV. It should be noted that the activation energy of this salt is the smallest among the series of $[Pt(ox)_2]^{n-}$ complexes reported so far.

The insulating state of 1D platinum complexes such as KCP and $M_x[Pt(ox)_2]\cdot nH_2O$ is well understood by Peierls instability accompanying the CDW. The 1D conductors exhibit metal-to-insulator (M−I) transition associated with displacive lattice distortion, the wave vector of which is equal to $2k_F$ (k_F is the Fermi wave vector). k_F is related to DPO[3b] because DPO determines the Fermi level in the conduction band. According to the X-ray structural data for **1**, the molecular ratio of $[Cu(bpy)(H_2O)_n]^{2+}$ to $[Pt(ox)_2]^{1.71-}$ is 0.857, and DPO of the Pt atom is estimated to be 0.286. Therefore, the period of the superlattice along the 1D platinum chain is calculated to be $7b_0$ (= $2b_0$/DPO), where b_0 is the average value of the intrachain spacing of Pt ions. This result is consistent with the observation of Bragg spots corresponding to the 7-fold periodicity along the b axis in the oscillation photographs. Thus, the insulating (or semiconducting) phase of **1** is characterized by the commensurate Peierls state with the $2k_F$ period along the b axis.

Braude et al. mentioned that $M_x[Pt(ox)_2]\cdot nH_2O$ with a divalent metal can be divided into two classes on the basis of their structural and transport properties.[7b] In the metallic state, diffuse lines associated with the $2k_F$ anomaly were observed as the precursor effects of Peierls instability for all compounds. Two types of insulating states exist below the M−I transition temperature. In the case of M = Ni, Co, or Zn, the insulating phase has its origin in the ordering of cations, which is clearly distinct from the simple Peierls transition and referred to as "non-Peierls" transition. At much lower temperature, the cation superlattice is commensurate with the Peierls distortion, and the salt is transformed into the CDW state. In the other compounds (M = Fe, Mg, or Mn), the ordering of cations in the superlattice is incommensurate with the Peierls distortion and no CDW state is formed. In both cases, the cation ordering seems to play an important role in the M−I transition of $M_x[Pt(ox)_2]\cdot nH_2O$ with divalent countercations. In contrast, the simple Peierls transition, which is ascribed to condensation of the soft phonon in the 1D platinum chain at $2k_F$, is seen in $M_x[Pt(ox)_2]\cdot nH_2O$ with monovalent countercations (M = K or Rb).[16,17] In the case of **1**, unlike $M_x[Pt(ox)_2]\cdot nH_2O$ with the divalent countercation, no disorder existing at the cation sites was observed because of the different cation type $[Cu(bpy)(H_2O)_n]^{2+}$ and the insulating phase corresponds to the simple Peierls state, similar to the latter case.

To investigate interactions between conduction electrons and local spins, magnetoresistance measurement was carried out for **1** at 100 K along the 1D platinum chain direction in the presence of magnetic fields of up to 9 T applied perpendicular to the chain (see Supporting Information). No remarkable change in resistivity was observed on application of the magnetic field, suggesting no substantial interaction between conduction electrons and local spins, although the Cu^{II} ion was directly coordinated by the oxygen atom of the $[Pt(ox)_2]^{1.71-}$ anion. Temperature dependences of magnetoresistance were measured; reproducible data were, however, obtained because of the deterioration of the sample crystals due to release of water molecules.

Electrical Conductivity of Complex 2. Room-temperature electrical conductivity along the 1D platinum chain direction of **2** is 3 orders of magnitude smaller ($\sigma_{\|}$ = 1.3 × 10^{-3} S cm^{-1}) than that of **1**. The temperature dependence of

(17) (a) Kobayashi, H.; Shirotani, I.; Kobayashi, A.; Sasaki, Y. *Solid State Commun.* **1997**, *23*, 409−413. (b) Kobayashi, A.; Sasaki, Y.; Shirotani, I.; Kobayashi, H. *Solid State Commun.* **1998**, *29*, 635−656.

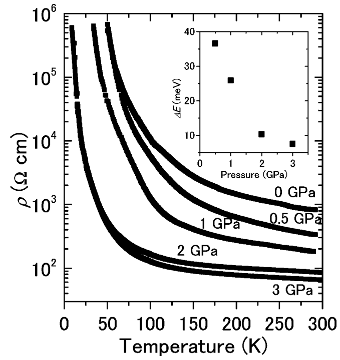

Figure 6. Temperature dependence of the resistivities of **1** under various pressures of up to 3 GPa. (Inset) Pressure dependence of the activation energy of **1**.

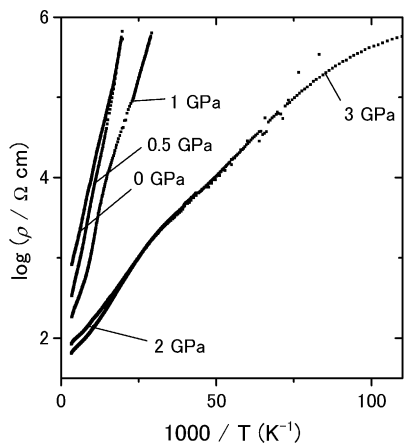

Figure 7. Arrhenius plot of resistivity under various pressures of up to 3 GPa for **1**.

the resistivity of **2** is shown in Figure 5. Similarly to **1**, the resistive behavior of **2** is semiconductive with an activation energy of 67 meV. The oxidation state of Pt ions in **2** is the same as that of the starting compound, $K_{1.62}[Pt(ox)_2]\cdot 2H_2O$; nevertheless, the conductivity of **2** is much smaller than that of α-$K_{1.62}[Pt(ox)_2]2H_2O$, the conductivity of which is $\sigma_{\|} = 10^2$ S cm^{-1} at room temperature. This can be explained by the fact that the inter-platinum distance ($d_{Pt2-Pt3} = 3.0082$ Å) of **2** is very large, compared with that of α-$K_{1.62}[Pt(ox)_2]$-$2H_2O$ ($d_{Pt-Pt} = 2.82$ Å). It is noted that the electrical conductivity of Rb salt is also very low ($\sigma_{\|} \approx 10^{-3}$ S cm^{-1}) which has the longest Pt−Pt distance of 3.015 Å.[17]

Electrical Conductivity of Complex 1 under Various Pressures. The pressure effect on electrical conductivity in **1** was investigated under various pressures of up to 3 GPa (Figure 6). Semiconductive behaviors were observed over the whole pressure range. The semiconducting behaviors were reduced with increasing pressure. The Arrhenius plot shows that the resistivity can be described by an activation-type conduction (Figure 7), and yields the activation energy of $\Delta E = 7.6-37$ meV. The pressure dependence of the activation energy, ΔE, shown in the inset of Figure 6, indicates that the ΔE value decreased to a minimum of 7.6 meV with increasing pressure, suggesting enhancement of electrical conduction with pressure application. The enhanced electrical conduction of **1** is due to increased intermetallic orbital overlaps. The conduction band of 1D Pt complexes such as KCP is generally composed of $5d_{z^2}$ orbitals of Pt ions,[4a,18] and application of pressure causes enhancement of intermetallic orbital overlaps of $5d_{z^2}$. It has been reported that the compression along the platinum chain direction is largest for Pt^{II} glyoximato complexes, $[Pt(dpg)_2]$,[19] [Pt-$(dmg)_2]$,[20] and $[Pt(bqd)_2]$[21] (dpg = diphenylglyoximato, dmg = dimethylglyoximato, and bqd = 1,2-benzoquinonegyloximato), and consequently, the electrical conductivities at room temperature are drastically increased with increasing pressure.

The resistive behavior is semiconductive without any remarkable anomalies at each pressure up to 3 GPa (Figure 7). Interactions of the localized d spins with the conduction electrons have been reported in the metal complex TPP[Fe^{III}-$(Pc)(CN)_2]_2$ (Pc = phthalocyanine and TPP^+ = tetraphenylphosphonium).[22] Each Pc ring in a 1D stack has a local spin of an Fe^{3+} ion. In this complex, the deviation from the activation-type conduction and enhancement of semiconducting behavior were observed below ca. 50 K, and giant negative magnetoresistance was observed. Therefore, the origin of the enhancement of the semiconducting phase could be explained by the spin scattering of itinerant π electrons by localized d spins through π−d interaction, and reduction of the spin scattering by magnetic field application leads to the negative magnetoresistance. In **1**, on the other hand, no such enhanced semiconducting phase was observed at low temperature, suggesting no substantial interactions between the conduction electrons and the local spins even with pressure application.

Conclusions

New conducting 1D complexes $[Cu(bpy)(H_2O)_n]_6[Pt(ox)_2]_7\cdot 7H_2O$ (n = 2, 3, or 4) (**1**) and $[Cu(bpy)(H_2O)_n]_8[Pt(ox)_2]_{10}\cdot 8H_2O$ (n = 3 or 4) (**2**) were synthesized, and their crystal structures and physical properties were investigated. In **1**, paramagnetic Cu^{II} ions are linked to conducting Pt chains via oxalate bridges, whereas no such links exist in **2**. In both salts the Pt ions are partially oxidized and form 1D anion chains along the *b* axis. The electrical conductivity of **2** along the 1D platinum chain direction ($\sigma_{\|} = 1.3 \times 10^{-3}$ S cm^{-1}) is much lower than that of **1** ($\sigma_{\|} = 0.9-0.5$ S cm^{-1}), which is due to the longer intrachain Pt−Pt distance in **2**. Complex **1** shows semiconducting behavior with an activation energy of 29 meV, which is the smallest among the electrical conducting $[Pt(ox)_2]^{n-}$ complexes hitherto known. The gap opening at the Fermi level in the conduction band is explained by Peierls instability leading to the CDW state. The 7-fold superstructure of **1** was confirmed by X-ray oscillation photographs and is in agreement with the period of the Peierls distortion estimated from the degree of partial

(18) Minot, M. J.; Perlstein, J. H. *Phys. Rev. Lett.* **1971**, *26*, 371−373.
(19) Shirotani, I.; Hayashi, J.; Takeda, K. *Mol. Cryst. Liq. Cryst.* **2005**, *442*, 157−166.
(20) Takeda, K.; Shirotani, I.; Yakushi, K. *Chem. Mater.* **2000**, *12*, 912−916.
(21) Takeda, K.; Shirotani, I.; Sekine, C.; Yakushi, K. *J. Phys.: Condens. Matter* **2000**, *12*, L483-L488.
(22) (a) Hanasaki, N.; Tajima, H.; Matsuda, M.; Naito, T.; Inabe, T. *Phys. Rev. B* **2000**, *60*, 5839−5842. (b) Matsuda, M.; Naito, T.; Inabe, T.; Hanasaki, N.; Tajima, H.; Otsuka, T.; Awaga, K.; Narymbetov, B.; Kobayashi, H. *J. Mater. Chem.* **2000**, *10*, 631−636.

oxidation. Magnetoresistance measurements at ambient pressure indicate no interactions of the conduction electrons in the Pt chain with the local spins on Cu^{II} ions. The resistivity decreased with application of hydrostatic pressures of up to 3 GPa, which is due to the enhanced intermolecular overlap integrals between the adjacent Pt ions by reducing the Pt−Pt distance. The absence of any distinct anomalies in the temperature dependence of resistivity under pressures of up to 3 GPa indicates no substantial interactions of the conduction electrons with the local spins even with pressure application. The activation energy is decreased with increasing pressure to 7.6 meV at 3 GPa. It is therefore significant to investigate transport properties including interactions of the conduction electrons with the local spins in this system under high pressures.

Acknowledgment. This work was supported by the COE and TARA projects in the University of Tsukuba and by a Grant-in-Aid for Scientific Research from the Ministry of Education, Culture, Sports, Science and Technology, Japan.

Supporting Information Available: X-ray crystallographic files in CIF format of **1** and **2**, and plot of magnetoresistance vs magnetic field for **1**. This material is available free of charge via the Internet at http://pubs.acs.org.

IC0607742